

Pushing run-and-tumble particles through a rugged channel

Bram Bijmens and Christian Maes

Instituut voor Theoretische Fysica, KU Leuven *

We analyze the case of run-and-tumble particles pushed through a rugged channel both in the continuum and on the lattice. The current characteristic is non-monotone in the external field with (1) the appearance of a current and nontrivial density profile even at zero field for asymmetric obstacles, (2) the current decreasing with persistence at small field and increasing with persistence at large field. Activity in terms of self-propulsion increases the maximal current and postpones dying. We give an effective theoretical description with wider validity.

I. INTRODUCTION

A nonequilibrium system, be it transient or stationary driven, is very sensitive to time-symmetric constraints and obstacles. Kinetic constraints or disorder indeed influence relaxation, diffusion and transport even for independent particles. For transport in out-of-equilibrium systems, even at small (and even zero) external driving, the frenetic contribution complements entropic considerations (as in the fluctuation–dissipation relation) to enter crucially in the current characteristic [1, 2]. Examples where the response to external fields, temperature or chemical affinities show negative differential susceptibility include [3–9]. In the present paper we revisit the set up of [3, 4] but for active particles as studied before e.g. also in [10–15]: how does the current characteristic change as a function of the persistence?

Active matter consists of self-propelled particles, characterized by a coupling between motion and an internal degree of freedom, quantified by persistence [16–20]. Their dynamics model bacteria-motion and nanomotors or active colloids for their locomotion, possibly showing collective effects such as flocking or phase separation [21–26]. Also individually they differ in many ways from their passive counterparts [27–29]. The models are characterized

*Electronic address: christian.maes@kuleuven.be

as overdamped motion, while being nonMarkovian in the position variable by the presence of colored noise.

Pushing active particles can be understood in various ways. We use the more neutral words of “pumping” or “pushing” to include janus-particles or active colloids but there are many specific ways in which also living organisms may respond to a signal and hence introduce bias into their movement [30]. We think about a fixed sensory gradient where a direction is preferred and remains the same for all individuals at all locations in space (e.g. from gravity). Or, when animals search for food, the direction may be taken of a target or source fixed in space.

As a model for self-propelled colloids, we take run-and-tumble particles (RTP), mimicking a behavior observed in chemotactic bacteria [31]. We have no very specific biological application in mind however, and we can as well take active colloids as susceptible to a global external driving as today can be realized in many ways. For a related approach and type of problem, see e.g. [32] showing glassy behavior in an active model. That is a form of kinetic arrest which is not unlike the trapping behavior we study in the present behavior, except that interactions will play no role here. It is the roughness of the channel that creates possible trapping.

Recently, there have appeared a growing number of studies of active systems exposed to disorder and obstacles, with [33] studying the influence of heterogeneity on large-scale collective properties, similarly for [34, 35] on flocking behavior and [10, 11, 36] for active particles running in a landscape of obstacles, typically randomly-placed disks, and [37–42] investigating diffusion properties of self-propelled particles in crowded or complex environments. Periodic arrays of obstacles were considered for (artificial) microswimmers in [43] and transport for active particles in periodic porous media was characterized in [12], for periodic arrays (for active Brownian particles) in [13–15]. In particular we mention [44, 45] for important new directions and [46] for modifier activation–inhibition switching in enzyme kinetics. Non-Boltzmann steady distribution and clustering have been studied for RTP in [17, 47–50]. New in the present paper is the study on the discrete lattice, incorporating the external field and activity at the same time, plus a general effective analysis able to summarize the properties of the rough substrate in terms of an effective mobility.

The plan is as follows: in the next section, we specify the question, after which we present

an effective dynamics to predict the main features of RTP-particles being pushed through a rough (but general) channel. Section III describes the model dynamics more specifically in the continuum and on the discrete lattice through a channel with obstacles. The obstacles lead (possibly) to trapping, as has been analyzed in various scenarios for passive particles. In Section IV we present the results of simulations, where the main output is the current characteristic, function of the external field, and how it depends on persistence. Section V concludes with the discussion, also with reference to the predictions in Section II.

II. QUESTION AND EFFECTIVE ANALYSIS

Active particles in a constant external field have been mostly considered for the problem of sedimentation. The experimental system is for example treated by Palacci *et al.*, [51]. Enculescu and Stark [52] considered active Brownian motion with an external time-independent constant force, studying sedimentation. Tailleur and Cates [53] showed that for the run-and-tumble model the stationary state distribution in a linear potential has the exponential form. For that model, a closed form of the stationary state distribution has been derived by Szamel in [54]. In the present paper we investigate the current for RTP-motion driven through a rough periodic channel, where the two-dimensional aspect matters for the placement of obstacles.

In this Section, we restrict ourselves to continuous space. (The aspects related to modeling RTP on the lattice in an external field will be given in Section III B.)

Run-and-tumble particles run on straight lines interrupted by tumbling at exponential times. At tumbling a new random direction is chosen. In an external field ε pointing in the x -direction with unit vector $\hat{\mathbf{e}}_x$, the two-dimensional position \vec{r}_t changes in time t following the differential equation

$$\dot{\vec{r}}_t = c \hat{\sigma}_t + \varepsilon \hat{\mathbf{e}}_x \quad (1)$$

where $c > 0$ is the amplitude of the noise $\hat{\sigma}_t$ which is itself a Markov process taking values in the space of unit-vectors (points on the circle):

$$\hat{\sigma}_t = \cos \theta_t \hat{\mathbf{e}}_x + \sin \theta_t \hat{\mathbf{e}}_y \quad (2)$$

with angle θ_t undergoing a jump process with constant rate $k(\theta, \theta') = a$. In other words,

at tumbling times, the particle randomly chooses a new angle to run. The particle feels the direction and stimulus intensity ε at every single point but its tumbling rate a is unaffected. We think of a channel, periodic along the x -direction, where the interior surface is not smooth. We ask for the stationary particle current and how it gets influenced by c and a and the channel properties. In Section III we will choose for hooks that block the motion. In general the dynamics (1) must be supplemented with boundary conditions indeed, but next we assume an effective one-dimensional and translation-invariant model where the roughness is replaced by a mobility μ .

Consider then the effective one-dimensional dynamics

$$\dot{x}_t = \psi(c\sigma_t + \varepsilon) \quad (3)$$

where $\sigma_t = \pm 1$ flips at rate a , and for $\psi(E) = E\mu(E)$ when the force is E , where the mobility $\mu(E)$ depends on the persistence and on the architecture of the unit cell. The idea is that (3) summarizes effectively the joint influence of the persistence and obstacles but coarse grained to the translation invariant scale. Note that the homogenized mobility μ refers to the current in the positive x -direction and needs not be symmetric at all, as it summarizes the spatial escape rate and roughness need not be symmetric.

For computing the current we go to the Master equation for (3),

$$\begin{cases} \partial_t \rho_+(x) = -\psi(c + \varepsilon) \partial_x \rho_+(x) - a(\rho_+(x) - \rho_-(x)) \\ \partial_t \rho_-(x) = -\psi(-c + \varepsilon) \partial_x \rho_-(x) + a(\rho_+(x) - \rho_-(x)) \end{cases} \quad (4)$$

where ρ_{\pm} represents the density where $\sigma_t = \pm 1$. Defining $\rho(x) = \rho_+(x) + \rho_-(x)$ for the total particle density and $m(x) = \rho_+(x) - \rho_-(x)$ for the chirality, we get

$$\begin{cases} \partial_t \rho(x) = -\frac{1}{2}[\psi(c + \varepsilon) - \psi(-c + \varepsilon)] \partial_x m(x) - \frac{1}{2}[\psi(c + \varepsilon) + \psi(-c + \varepsilon)] \partial_x \rho(x) \\ \partial_t m(x) = -\frac{1}{2}[\psi(c + \varepsilon) - \psi(-c + \varepsilon)] \partial_x \rho(x) - \frac{1}{2}[\psi(c + \varepsilon) + \psi(-c + \varepsilon)] \partial_x m(x) - 2a m(x) \end{cases}$$

On the other hand, writing $\psi_+ = \psi(c + \varepsilon)$, $\psi_- = \psi(-c + \varepsilon)$,

$$\partial_{tt}^2 \rho = \frac{1}{4}(\psi_+ - \psi_-)^2 \partial_{xx}^2 \rho + \frac{1}{4}(\psi_+^2 - \psi_-^2) \partial_{xx}^2 m + a(\psi_+ - \psi_-) \partial_x m - \frac{1}{2}(\psi_+ + \psi_-) \partial_{xt}^2 \rho$$

and hence

$$\partial_{tt}^2 \rho + 2a \partial_t \rho = \frac{1}{4}(\psi_+ - \psi_-)^2 \partial_{xx}^2 \rho + \frac{1}{4}(\psi_+^2 - \psi_-^2) \partial_{xx}^2 m - \frac{1}{2}(\psi_+ + \psi_-) \partial_{xt}^2 \rho - a(\psi_+ + \psi_-) \partial_x \rho$$

We still need

$$\partial_{xt}^2 \rho = -\frac{1}{2}(\psi_+ - \psi_-)\partial_{xx}^2 m - \frac{1}{2}(\psi_+ + \psi_-)\partial_{xx}^2 \rho$$

to eliminate $\partial_{xx}^2 m$, after which we find the modification of the telegraph equation,

$$\partial_{tt}^2 \rho + 2a\partial_t \rho + \frac{1}{2}(\psi_+ + \psi_-)\partial_{xt}^2 \rho = -\psi_+\psi_-\partial_{xx}^2 \rho - a(\psi_+ + \psi_-)\partial_x \rho \quad (5)$$

purely in terms of the particle density $\rho(x, t)$. Note that when $\mu(E) = 1$, $\psi_+ = c + \varepsilon$, $\psi_- = -c + \varepsilon$ (no obstacles), the mobility does not depend on the force and the equations (3)–(5) become

$$\begin{aligned} \frac{d}{dt}(x - \varepsilon t) &= c \sigma_t \\ \partial_{tt}^2 \rho + (2a + \varepsilon \partial_x)(\partial_t \rho + \varepsilon \partial_x \rho) &= c^2 \partial_{xx}^2 \rho \end{aligned} \quad (6)$$

(hyperbolic when $4(\varepsilon^2 - c^2) < \varepsilon^2$). Those do not yet take into account boundary conditions (interior of the channel). Such one-dimensional models with bias and persistence have been studied analytically in [55]. We remember from there that the current as well as the diffusion coefficient are enhanced by persistence.

Continuing with (5) we calculate the stationary current

$$j = \lim_t \frac{d}{dt} \int dx \rho_t(x) x$$

by multiplying (5) with x and integrating over x . The mean velocity $v_t = \frac{d}{dt} \int dx \rho_t(x) x$ satisfies

$$\partial_t v_t + 2a v_t = a(\psi_+ + \psi_-), \quad v_t = e^{-2at} v_0 + \frac{\psi_+ + \psi_-}{2}(1 - e^{-2at})$$

which asymptotically in time t becomes

$$\begin{aligned} v_t \rightarrow j &= \frac{\psi(c + \varepsilon) + \psi(-c + \varepsilon)}{2} \\ &= \frac{c}{2} [\mu(c + \varepsilon) - \mu(-c + \varepsilon)] + \frac{\varepsilon}{2} [\mu(c + \varepsilon) + \mu(-c + \varepsilon)] \end{aligned} \quad (7)$$

The current-characteristic $j = j(\varepsilon; c, a)$ is thus largely decided by the behavior of the effective mobility, which also depends on the persistence a (and on the local roughness). There are in fact two other length scales besides L , which we can take as the size of the unit cell or obstacles: there is ε/a which is the bias length and c/a which is the persistence length.

Let us first take $c \gg \varepsilon$. We see that $j > 0$ unless $\mu(\varepsilon - c)$ is large enough. For example, for zero external field $\varepsilon = 0$, $\mu(-c) > \mu(c)$ yields a negative current $j(\varepsilon = 0) < 0$ at zero field,

which is very well possible if escape opposite to the field becomes easier than with the field. Larger persistence is then expected to increase the difference $\mu(-c) - \mu(c)$ which lowers the current at small bias.

For large $\varepsilon \gg c$ we have $j \simeq \varepsilon\mu(\varepsilon)$, and the decay of the mobility in ε decides the characteristic for large pumping. We may expect that if there is a horizon of unblocked escape, larger persistence (in that direction) increases $\mu(\varepsilon)$, and more for larger c .

We see next more specifically for a periodic channel with obstacles how the predictions of the above effective analysis get realized, in particular when the unit cell is asymmetric.

III. MODEL WITH OBSTACLES

We restrict ourselves to two types of obstacles, both time-symmetric but one which is spatially asymmetric (with one type of hook) and one which is spatially symmetric. The space is quasi-one dimensional, either continuous, in Section III A, or discrete, in Section III B. See Fig. 1 for the setup of the rough channel, showing three unit cells. We have also indicated the direction of the nonconservative external field of strength ε .

In the numerical simulations, time is discrete with steps of size Δt . The current j is measured during an interval $[0, t_{\max}]$ after the system had time to relax. The stationary current is then obtained as

$$j = \frac{\phi_r - \phi_\ell}{t_{\max}} \quad (8)$$

where ϕ_r and ϕ_ℓ are the number of particles leaving the unit cell through the right, respectively the left boundary of the unit cell. Starting positions of N particles are chosen randomly within the unit cell and evolve independently.

A. Continuum model

The motion (1) is supplemented with boundary conditions. We refer to Figs. 1 for the basic architectures that are repeated periodically. For the obstacles (solid lines in the figures) the boundary conditions are hovering, meaning that when a particle hits these boundaries it will continue by keeping (only) its velocity component parallel to the surface. Particles cannot move through obstacles. For the rest, when not at an obstacle, boundary

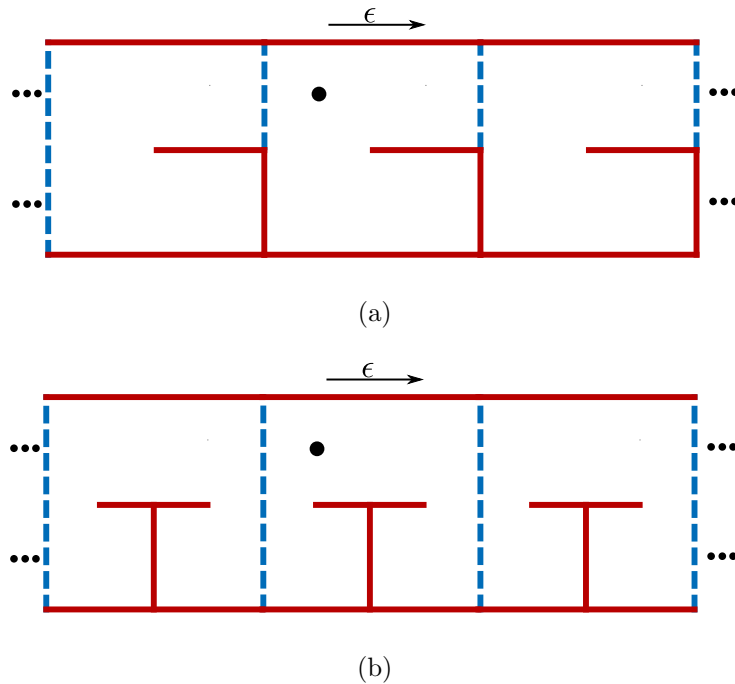


FIG. 1: Periodic channel with obstacles in the form of hooks **(a)** asymmetric hook and **(b)** symmetric hook. Solid lines (red) are obstacles, the dashed lines (blue) only indicate the boundaries of the unit cells.

conditions are periodic in the (horizontal) x -direction: if a particle leaves the unit cell at these boundaries it enters the unit cell at the opposing side.

The simulations use a unit cell with sides of unit length, the walls of the obstacles have half the length of the cell making them span over one-fourth of the area. Other parameters are $\Delta t = 0.001$, $t_{\max} = 500$, $N = 10000$ and $c = 1$ unless stated otherwise.

B. Discrete model

For run-and-tumble motion on the discrete lattice, we deal with a random walk showing persistence and subject to an external bias [30, 55, 56]. Hopping is between lattice sites except that particles cannot cross the walls (the solid (red) lines in Fig. 2). The unit cell is again repeated periodically. Study of the current-characteristic for active particles on a discrete lattice with obstacles is new and requires some new elements to take care of.

The run-and-tumbling follows the same idea as in the continuum case but com-

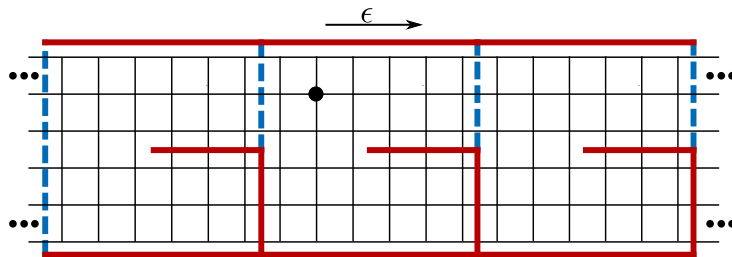


FIG. 2: Setup for the discrete lattice model with a hook at the right. The same is done for the symmetric case of Fig. 1(b).

binning persistence with bias in a continuous time random walk in two dimensions requires more explanations. The (internal) spin direction also becomes discrete and can either point right, left, up or down. The tumbling is still uniformly to one of the other directions with a rate a , i.e., with uniform and symmetric transition rates $k(\text{right},\text{left}) = k(\text{right},\text{up}) = k(\text{right},\text{down}) = \dots = a$. The particle is persistent in one of the four directions and is subject also to an external field ε pointing to the right in the (horizontal) x -direction. We now specify the hopping rates. There will be each time four hopping rates, and each is set to zero when an obstacle prevents the hopping (see again Fig. 2). The hopping rates depend on the current direction of persistence (with amplitude c) and the external field ε .

To better understand the logic of the formulæ that follow, we first consider a one-dimensional integer lattice with sites j , for modelling a run-and-tumble particle in an external field (without obstacles). For that purpose we propose the following rates.

When the direction of persistence is to the right (subscript $+$), we take rates

$$k_+(j, j+1) = \exp b_+, \quad k_+(j, j-1) = \exp -b_+$$

and similarly

$$k_-(j, j+1) = \exp b_-, \quad k_-(j, j-1) = \exp -b_-$$

for the hopping rates when the persistence is to the left (with subscript $-$). The master equation for the density $\rho_+(j)$, respectively $\rho_-(j)$ is

$$\begin{cases} \partial_t \rho_+(j) = e^{b_+} (\rho_+(j-1) - \rho_+(j)) + e^{-b_+} (\rho_+(j+1) - \rho_+(j)) - a (\rho_+(j) - \rho_-(j)) \\ \partial_t \rho_-(j) = e^{b_-} (\rho_-(j-1) - \rho_-(j)) + e^{-b_-} (\rho_-(j+1) - \rho_-(j)) - a (\rho_-(j) - \rho_+(j)) \end{cases} \quad (9)$$

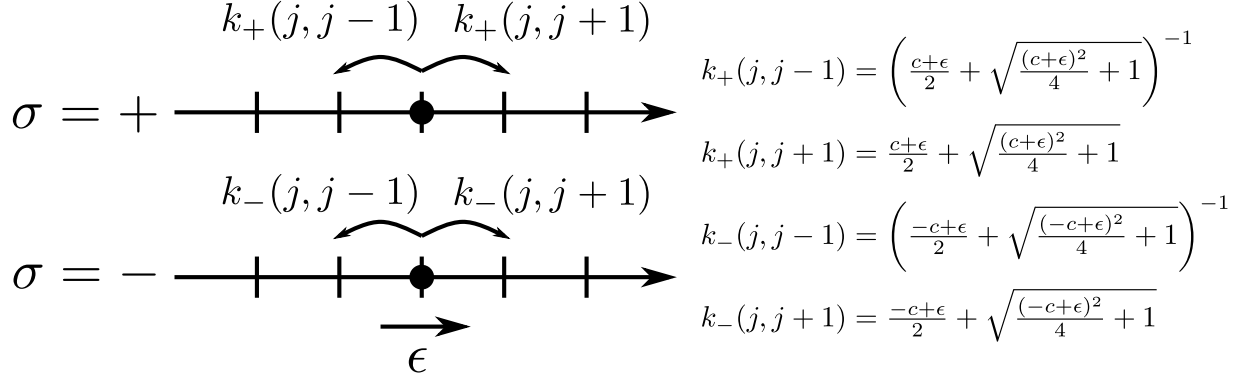


FIG. 3: Setup for a one-dimensional RTP in a field ϵ .

Clearly then, we should take $2 \sinh b_+ = c + \epsilon$ and $2 \sinh b_- = -c + \epsilon$ for mimicking the run-and-tumble motion $\dot{x}_t = c\sigma_t + \epsilon$ on \mathbb{R} , with $\sigma_t = \pm 1$ tumbling at rate a . Observe that on the lattice, particles are still allowed to go against the direction of persistence in the same way as they can go against the external field. In the continuum limit (scaling time and space in the same way) we obtain the correct run-and-tumble dynamics. There exist other versions of lattice dynamics of run-and-tumble particles, in particular for $\epsilon = 0$ where we can simply take one-way rates depending on the direction of persistence; see for example [55, 57]. However, in our model, we can easily put $c = 0$ and keep the motion of a biased random walker for $\epsilon \neq 0$.

We extend the above idea to the two-dimensional lattice, e.g. in Fig.2. It is important that when the external field is zero $\epsilon = 0$ the hopping rates in the three other directions from the direction of persistence are just equal. We now put subscripts r, ℓ, u, d for the direction of persistence, indicating right, left, up or down respectively. We then denote $p = r, \ell, u, d$ for the persistence direction, and get the hopping rates

$$k_p(j, j + \hat{e}_x) = e^{\alpha_p}, \quad k_p(j, j - \hat{e}_x) = e^{\beta_p}, \quad k_p(j, j + \hat{e}_y) = e^{\gamma_p}, \quad k_p(j, j - \hat{e}_y) = e^{\lambda_p}$$

with

$$\left\{ \begin{array}{l} \sinh \alpha_r = \frac{c+\epsilon}{2} \\ \sinh \beta_r = -\frac{c+\epsilon}{2} \\ \sinh \gamma_r = \frac{-c}{2} \\ \sinh \lambda_r = \frac{-c}{2} \end{array} \right. , \left\{ \begin{array}{l} \sinh \alpha_\ell = \frac{-c+\epsilon}{2} \\ \sinh \beta_\ell = -\frac{-c+\epsilon}{2} \\ \sinh \gamma_\ell = \frac{-c}{2} \\ \sinh \lambda_\ell = \frac{-c}{2} \end{array} \right. , \left\{ \begin{array}{l} \sinh \alpha_u = \frac{-c+\epsilon}{2} \\ \sinh \beta_u = -\frac{c+\epsilon}{2} \\ \sinh \gamma_u = \frac{c}{2} \\ \sinh \lambda_u = \frac{-c}{2} \end{array} \right. , \left\{ \begin{array}{l} \sinh \alpha_d = \frac{-c+\epsilon}{2} \\ \sinh \beta_d = -\frac{c+\epsilon}{2} \\ \sinh \gamma_d = \frac{-c}{2} \\ \sinh \lambda_d = \frac{c}{2} \end{array} \right.$$

explicitly in terms of the physical amplitudes c and ϵ . The above may seem complicated updating formulæ but we claim they are the physically correct ones for RTP in an external field on a 2dimensional lattice.

Again the unit cell has sides of unit length, there are 10 rows and 10 columns of lattice sites, leading to an inter site distance $\delta_x = \delta_y = 0.1$. The walls are placed between lattice points prohibiting hopping over them. The asymmetric hooks consist of a barrier between columns 10 and 1 for the 5 bottom rows of the lattice and one in columns 5 to 10 between rows 5 and 6. The symmetric hooks, on the other hand, have one barrier between columns 5 and 6 for rows 1 to 5 and a second one above columns 3 to 8 between row 5 and 6. The other parameters used in the simulations are $\Delta t = 0.01$, $t_{\max} = 500$, $N = 10000$ and $c = 0.5$ or 1 unless mentioned otherwise.

IV. RESULTS

The current characteristic gives the dependence of the stationary current on the external field ϵ , on the persistence time a^{-1} and on the coupling amplitude c .

Our findings are summarized in Figs. 4 for the continuum model and in Figs. 5 for the discrete case. To the left, we see the case for an asymmetric trap as in Fig. 1(a) and to the right for a spatially symmetric obstacle as in Fig. 1(b).

We find the following behavior (in the continuum and on discrete lattice):

1. For small enough (including zero) external field and for asymmetric trapping there appears a current opposite the external field. In fact, for zero field and in a closed box with asymmetric trapping there appears a density gradient.
2. There exists a threshold value $\epsilon_c > 0$ so that for $0 \leq \epsilon < \epsilon_c$ the current decreases with persistence time a^{-1} , and for $\epsilon_c < \epsilon$ the current increases with the persistence. This

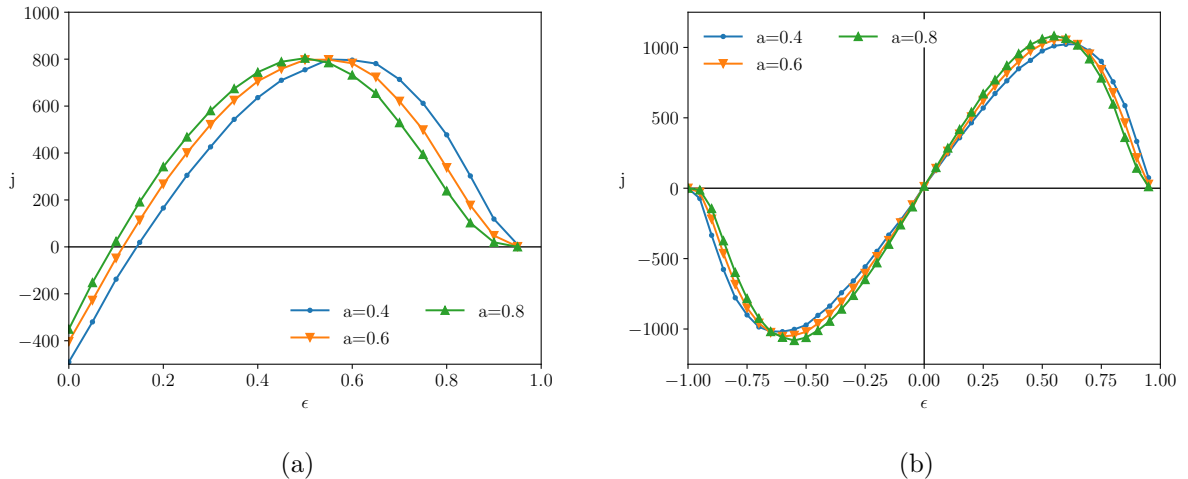


FIG. 4: The current-field characteristic for different persistence values in the continuum with $c = 1$. Left: asymmetric hook as in Fig. 1(a). Note the current is negative for zero field, and still lower for higher persistence at low bias, while the current increases with the bias at larger field. Right: symmetric hook as in Fig. 1(b). The current depends less on the persistence at small field values, but still increases with persistence at large fields.

ε_c depends on the coupling amplitude c and occurs around $\varepsilon = O(c)$.

For example, compared to the passive case, the current in the active case is first smaller and later gets larger. The dying of the current is postponed longer for greater activity.

3. The effect of persistence becomes more important for larger speed c . For fixed persistence, the current grows with c but the maximal current is not monotone in c .

V. DISCUSSION

We refer to our findings in the previous section, and we discuss how they are clarified from the effective model in Section II.

1. Asymmetric traps yield a nonzero current in zero fields. The active system is clearly not in equilibrium even at $\varepsilon = 0$. The current generation (opposite to the trap) is similar to what happens in the case of the Parrondo paradox or for flashing ratchets where the nonequilibrium condition conspires with asymmetry [58–60]. It was also found recently in [45] for active particles. Here the point is foremost that particles

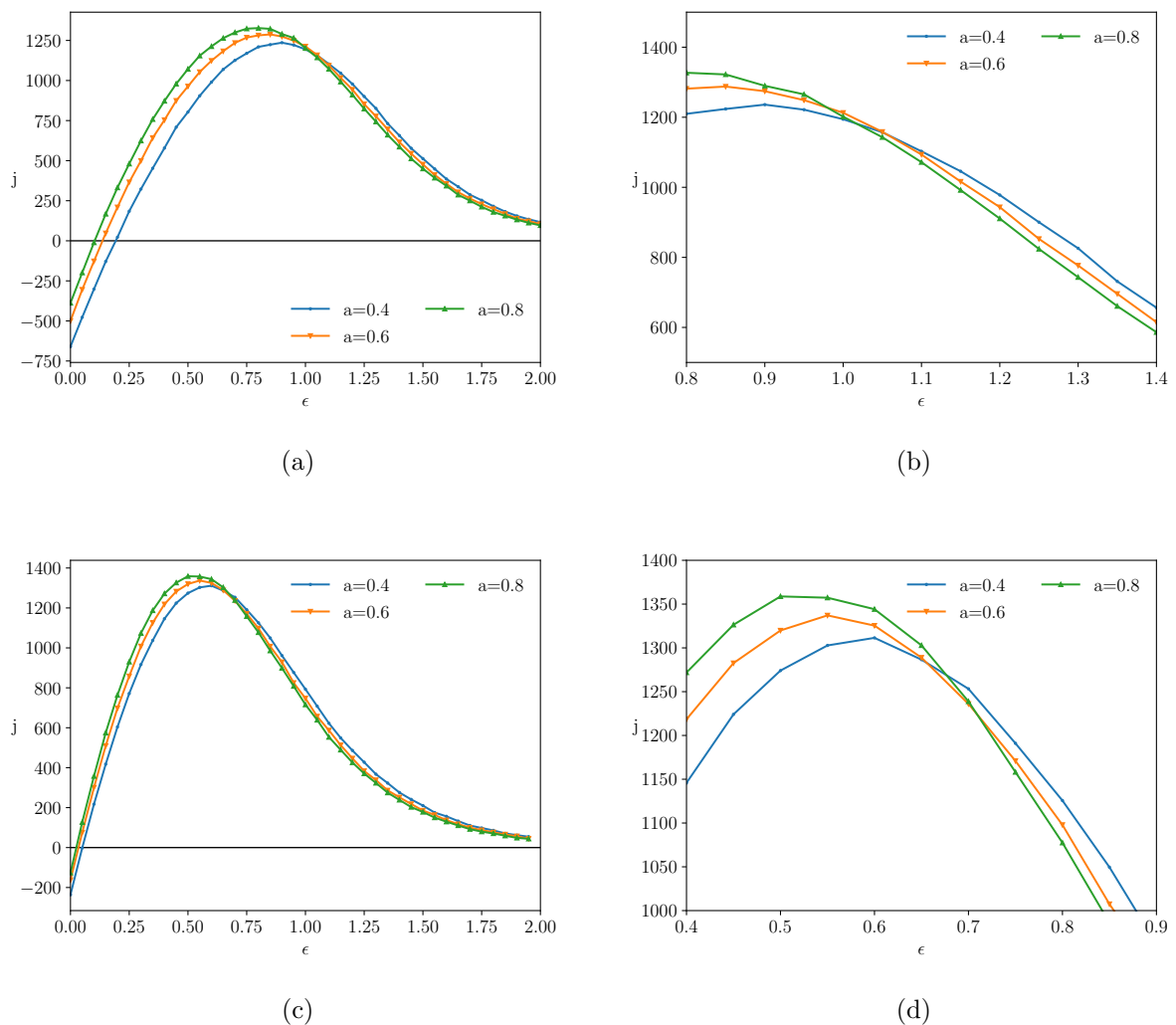


FIG. 5: The current-field characteristic for different persistence values for the asymmetric hook as in Fig. 1(a). $c = 1$ for (a) and (b) and $c = 0.5$ for (c) and (d). Left: The current characteristic is similar to the continuum Fig. 4(a), except in the large field regime where persistence matters less. Right: The current switches from decreasing to increasing with the persistence time a^{-1} , around some value ϵ_c .

starting inside the trap typically contribute to the current in the opposite direction; see Fig. 7. Particles in the trap tend to leave the unit cell to the left, as they need persistence in a direction opposite the wall, ending up in the left half of the cell. The analytical analogue is that $\mu(-c) > \mu(c)$ in (7) and as announced there.

2. The initial decrease in the small-field current (including $j_{\epsilon=0}$) is related to the previous

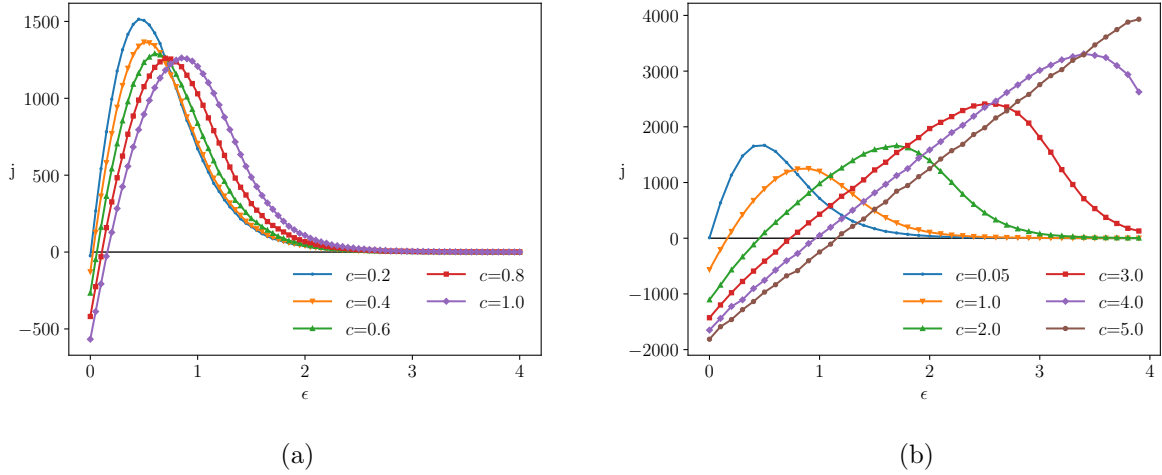


FIG. 6: The current-field characteristic for different coupling amplitude c at $a = 0.5$ on the lattice. The field at which the current is maximal increases with c and the maximum value is smallest for $c = 1$.

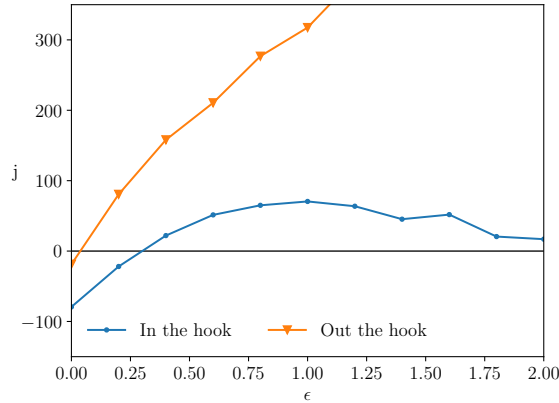


FIG. 7: RTP trapped in the right-hook of Fig. 2 typically leave the unit cell to the left, especially at high persistence (here: $a = 0.5$ and $c = 1$). To evaluate the effect of the starting position, the current (8) is only measured until $t_{\max} = 10$.

remark, as for small field and higher persistence, there is a substantial contribution of negative flux due to particles that are trapped. For higher persistence, the particles may go for a longer time against the field and it thus takes a larger field to fully trap them. As $a \rightarrow \infty$ the particle becomes passive and $j_{\epsilon=0} = 0$.

3. For large external field ε , the effective field $\varepsilon \pm c$ is always positive and trapping occurs

finally inside the hook. The current goes down exponentially fast in ε as the mobility $\mu(E)$ is exponentially small in E as for the passive case [4]. What we see here in general is nonequilibrium response where a positive correlation between current and frenesy in the *original* dynamics produces a negative contribution; see e.g. [61]. From the results in the present paper we conclude that persistence in self-propulsion is able to postpone the trapping-effect. At large enough pumping, RTP obtain an increased current for higher activity. Refinements where the tumbling rate depends on the neighborhood of an obstacle or on the direction of the external field [31] can be considered in further studies.

Acknowledgment: Bram Bijmens is grateful for the opportunity of the student internship at the Institute for Theoretical Physics in Leuven, during which the present study was completed.

-
- [1] C. Maes, Frenesy: Time-symmetric dynamical activity in nonequilibria. *Phys. Rep.* **850**, 1–33 (2020).
 - [2] C. Maes, *Non-Dissipative Effects in Nonequilibrium Systems*. SpringerBriefs in Complexity, 2018.
 - [3] R.K.P. Zia, E.L. Præstgaard and O.G. Mouritsen, Getting more from pushing less: Negative specific heat and conductivity in nonequilibrium steady states. *Am. J. Phys.* **70**, 384 (2002).
 - [4] P. Baerts, U. Basu, C. Maes and S. Safaverdi, The frenetic origin of negative differential response. *Phys. Rev. E* **88**, 052109 (2013).
 - [5] R.L. Jack, D. Kelsey, J.P. Garrahan and D. Chandler, Negative differential mobility of weakly driven particles in models of glass formers. *Phys. Rev. E* **78**, 011506 (2008).
 - [6] O. Bénichou, P. Illien, G. Oshanin, A. Sarracino and R. Voituriez. Microscopic theory for negative differential mobility in crowded environments. *Phys. Rev. Lett.* **113**, 268002 (2014).
 - [7] G. Falasco, T. Cossetto, E. Penocchio and M. Esposito, Negative differential response in chemical reactions. arXiv:1812.11245v1 [cond-mat.stat-mech].
 - [8] C. Reichhardt and C.J.O. Reichhardt, Directional Clogging and Phase Separation for Disk-

- Flow Through Periodic and Diluted Obstacle Arrays. arXiv:2009.11372v1 [cond-mat.soft].
- [9] A. Sarracino, F. Cecconi, A. Puglisi and A. Vulpiani, Nonlinear response of inertial tracers in steady laminar flows: differential and absolute negative mobility. *Phys. Rev. Lett.* **117**, 174501 (2016).
 - [10] C. Reichhardt and C. J. O. Reichhardt, Clogging and depinning of ballistic active matter systems in disordered media. *Phys. Rev. E* **97**, 052613 (2018).
 - [11] C. Reichhardt and C. J. O. Reichhardt, Active matter transport and jamming on disordered landscapes. *Phys. Rev. E* **90**, 012701 (2014).
 - [12] R. Alonso-Matilla, B. Chakrabarti and D. Saintillan, Transport and dispersion of active particles in periodic porous media. *Phys. Rev. Fluids* **4**, 043101 (2019).
 - [13] S. Pattanayak, R. Das, M. Kumar and S. Mishra, Enhanced dynamics of active Brownian particles in periodic obstacle arrays and corrugated channels. *Eur. Phys. J. E* **42**, 62 (2019).
 - [14] C. Kreuter, U. Siems, P. Nielaba, P. Leiderer and A. Erbe, Transport phenomena and dynamics of externally and self-propelled colloids in confined geometry. *Eur. Phys. J. Special Topics* **222**, 2923 (2013).
 - [15] H. E. Ribeiro, W. P. Ferreira and F. Q. Potiguar, Trapping and sorting of active matter in a periodic back-ground potential. *Phys. Rev. E* **101**, 032126 (2020).
 - [16] P. Romanczuk, M. Bar, W. Ebeling, B. Lindner and L. Schimansky-Geier, Active Brownian particles. *Eur. Phys. J. Special Topics* **202**, 1 (2012).
 - [17] C. Bechinger, R. Di Leonardo, H. Lowen, C. Reichhardt, G. Volpe and G. Volpe, Active particles in complex and crowded environments. *Rev. Mod. Phys.* **88**, 045006 (2016)
 - [18] S. Ramaswamy, Active matter. *J. Stat. Mech.* 054002 (2017).
 - [19] E. Fodor, and M.C. Marchetti, The statistical physics of active matter: from self-catalytic colloids to living cells. *Physica A* **504**, 106 (2018).
 - [20] G. Gompper *et al.*, The 2020 motile active matter roadmap. *J. Phys.: Condens. Matter* **32**, 193001 (2020).
 - [21] J. Toner, Y. Tu, S. Ramaswamy, Hydrodynamics and phases of flocks. *Ann. of Phys.* **318**, 170 (2005).
 - [22] N. Kumar, H. Soni, S. Ramaswamy, A.K. Sood, Flocking at a distance in active granular matter. *Nature Comm.* **5**, 4688 (2014).
 - [23] J. Schwarz-Linek, C. Valeriani, A. Cacciuto, M. E. Cates, D. Marenduzzo, A. N. Morozov,

- W. C.K. Poon, Phase separation and rotor self-assembly in active particle suspensions. *Proc. Natl. Acad. Sci. USA* **109**, 4052 (2012).
- [24] G. S. Redner, M. F. Hagan, and A. Baskaran, Structure and Dynamics of a Phase-Separating Active Colloidal Fluid. *Phys. Rev. Lett.* **110**, 055701 (2013).
- [25] J. Stenhammar, R. Wittkowski, D. Marenduzzo, and M. E. Cates, Activity-Induced Phase Separation and Self-Assembly in Mixtures of Active and Passive Particles. *Phys. Rev. Lett.* **114**, 018301 (2015).
- [26] M.E. Cates and J. Tailleur, Motility-Induced Phase Separation. *Annu. Rev. Condens. Matter Phys.* **6**, 219 (2015).
- [27] K. Malakar, V. Jemseena, A. Kundu, K. Vijay Kumar, S. Sabhapandit, S. N. Majumdar, S. Redner, A. Dhar, Steady state, relaxation and first-passage properties of a run-and-tumble particle in one-dimension. *JSTAT* 043215 (2018).
- [28] U. Basu, S. N. Majumdar, A. Rosso, G. Schehr, Active Brownian motion in two dimensions. *Phys. Rev. E* **98**, 062121 (2018).
- [29] T. Demaerel and C. Maes, Active processes in one dimension. *Phys. Rev. E* **97**, 032604 (2018).
- [30] E.A. Codling, M.J. Plank and S. Benhamou, Random walk models in biology. *J. R. Soc. Interface* **5**, 813–834 (2008).
- [31] H.C. Berg, *E. Coli in Motion*. Springer Verlag, Heidelberg, 2004.
- [32] L. Berthier and J. Kurchan, Non-equilibrium glass transitions in driven and active matter. *Nature Phys.* **9**, 310–314 (2013).
- [33] O. Chepizhko and F. Peruani, Active particles in heterogeneous media display new physics: existence of optimal noise and absence of bands and long-range order. *Eur. Phys. J. Spec. Top.* **224**, 1287–1302 (2015).
- [34] A. Morin, N. Desreumaux, J.-B. Caussin and D. Bartolo, Distortion and destruction of colloidal flocks in disordered environments. *Nature Phys.* **13**, 63–67 (2017).
- [35] D. A. Quint and A. Gopinathan, Topologically induced swarming phase transition on a 2D percolated lattice. *Phys. Biol.* **12**, 046008 (2015).
- [36] Cs. Sándor, A. Libál, C. Reichhardt and C. J. Olson Reichhardt, Dynamic phases of active matter systems with quenched disorder. *Phys. Rev. E* **95**, 032606 (2017).
- [37] A. Morin, D. Lopes Cardozo, V. Chikkadi and D. Bartolo, Diffusion, subdiffusion, and localization of active colloids in random post lattices. *Phys. Rev. E* **96**, 042611 (2017).

- [38] M. Zeitz, K. Wolff and H. Stark, Active Brownian particles moving in a random Lorentz gas. *Eur. Phys. J. E* **40**, 23 (2017).
- [39] T. Bertrand, Y. Zhao, O. Bènichou, J. Tailleur and R. Voituriez, Optimized diffusion of run-and-tumble particles in crowded environments. *Phys. Rev. Lett.* **120**, 198103 (2018).
- [40] O. Chepizhko and T. Franosch, Ideal circle microswimmers in crowded media. *Soft Matter* **15**, 452–461 (2019).
- [41] T. Bhattacharjee and S. S. Datta, Confinement and activity regulate bacterial motion in porous media. *Soft Matter* **15**, 9920 (2019).
- [42] T. Jakuszeit, O. A. Croze and S. Bell, Diffusion of active particles in a complex environment: Role of surface scattering. *Phys. Rev. E* **99**, 012610 (2019).
- [43] G. Volpe, I. Buttinoni, D. Vogt, H.-J. Kümmerer and C. Bechinger, Microswimmers in patterned environments. *Soft Matter* **7**, 8810–8815 (2011).
- [44] C. Reichhardt, C. J. O. Reichhardt, Directional Locking Effects for Active Matter Particles Coupled to a Periodic Substrate. arXiv:2008.05438v1 [cond-mat.soft].
- [45] C.J.O. Reichhardt and C. Reichhardt, Ratchet Effects in Active Matter Systems. *Annu. Rev. Condens. Matter Phys.* **8**, 51 (2017).
- [46] Hao Ge, Min Qian and Hong Qian, Stochastic theory of nonequilibrium steady states. Part II: Applications in chemical biophysics. *Physics Reports* **510**, 87–118 (2012).
- [47] A. Dhar, A. Kundu, S. N. Majumdar, S. Sabhapandit, G. Schehr, Run-and-tumble particle in one-dimensional confining potentials: Steady-state, relaxation, and first-passage properties. *Phys. Rev. E* **99**, 032132 (2019).
- [48] J. Tailleur and M. E. Cates, Statistical Mechanics of Interacting Run-and-Tumble Bacteria. *Phys. Rev. Lett.* **100**, 218103 (2018).
- [49] F. J. Sevilla, A. V. Arzola, E. P. Cital, Stationary superstatistics distributions of trapped run-and-tumble particles. *Phys. Rev. E* **99**, 012145 (2019).
- [50] E. Mallmin, R. A. Blythe, M. R. Evans, A comparison of dynamical fluctuations of biased diffusion and run-and-tumble dynamics in one dimension. *J. Phys. A: Math. Theor.* **52**, 425002 (2019).
- [51] J. Palacci, C. Cottin-Bizonne, C. Ybert, and L. Bocquet, Sedimentation and Effective Temperature of Active Colloidal Suspensions. *Phys. Rev. Lett.* **105**, 088304 (2010).
- [52] M. Enculescu and H. Stark, Active Colloidal Suspensions Exhibit Polar Order under Gravity.

- Phys. Rev. Lett. **107**, 058301 (2011).
- [53] J. Tailleur and M. E. Cates, Sedimentation, trapping, and rectification of dilute bacteria. Europhys. Lett. **86**, 60002 (2009).
- [54] G. Szamel, Self-propelled particle in an external potential: Existence of an effective temperature. Phys. Rev. E **90**, 012111 (2014).
- [55] N. Pottier, Analytic study of the effect of persistence on a one-dimensional biased random walk. Physica A **230**, 563–576 (1996).
- [56] C.S. Patlak, Random walk with persistence and external bias. Bull. Math. Biophys. **15**, 311–338 (1953).
- [57] R. Dandekar, S. Chakraborti and R. Rajesh, Hard core run and tumble particles on a one dimensional lattice. arXiv:2006.05980v1 [cond-mat.stat-mech].
- [58] J.M.R. Parrondo, Reversible ratchets as Brownian particles in an adiabatically changing periodic potential. Physical Review E **57**, 7297 (1998).
- [59] P. Hänggi and F. Marchesoni, Artificial Brownian motors: Controlling transport on the nanoscale. Rev. Mod. Phys. **81** (2009).
- [60] D. Cubero and F. Renzoni, *Brownian Ratchets: From Statistical Physics to Bio and Nanomotors*. Cambridge University Press, 2016.
- [61] C. Maes, Response theory: a trajectory-based approach. Frontiers in Physics, section Interdisciplinary Physics (2020).